Laser Bending of Thin Metal Sheets by Means of a Low Power CO_2 Laser

Gigliola Lubiano, Jorge A. Ramos[1]
Department of Mechanical and Metallurgical Engineering
Pontificia Universidad Catolica de Chile
Av. Vicuña Mackenna 4860 Casilla 306-Correo 22
Santiago - Chile

Johnathan Magee[2]
Laser Laboratory, Mechanical Engineering, Department of Engineering
University of Liverpool
Liverpool L69 3GH, United Kingdom

ABSTRACT

An experimental study of the deformation phenomena during laser bending of 0.5 mm metal sheets is presented here. The thermal gradient mechanism, i.e. ratio of the laser beam diameter to the sheet thickness less than unity, was used to bend the samples. The sheets, which are made of 304 stainless steel, 1100 aluminum and 1010 carbon steel, were scanned with a focused CO_2 laser beam for several times. Optical power of the laser ranged from 64 to 95 W and its maximum traverse speed was 15 mm/s. Results are presented as plots of the bending angle vs. number of scans (i.e. 2θ-N curves). Understanding of this novel forming process is crucial in order to find applications for it in the rapid prototyping field.

Introduction

Processing of materials using CO_2, Nd:YAG or diode laser beams is unique in that the energy required in any specific process can be delivered spatially and temporally over the surface of the material with high accuracy [1,2]. Among the laser processing techniques, laser bending has evolved as an important research activity in recent years [1,2,3,4]. It is a novel laser based technique, which bends wrought metal sheets by thermally induced stresses offering a "tool-less" bending process in contrast with mechanical methods. Large scale applications of laser bending may be found in shipbuilding and it has been applied successfully to the alignment of miniature structures in the microelectronics industry [4]. Laser bending of high strength titanium based superalloys sheets, as used in the aircraft industry, has also been achieved [5]. Recently, this

[1] e-mail: jramos@ing.puc.cl; jaramos@mail.utexas.edu
[2] e-mail: magee@mechnet.liv.ac.uk

bending process has emerged as a viable means of assisting conventional forming processes with geometrical accuracy related problems, however laser bending is still in its infancy in terms of accurate in-process control [6]. The process itself is slow and suitable for the production of "one of a kind" parts. Nonetheless, laser bending may run at lower costs than conventional bending (e.g. press break), since no expensive tooling is required and minimal clamping must be considered. One of the main tasks that still needs to be addressed and solved is the influence that the material properties have in the resulting bend angle [7,8]. In despite of these facts, rapid prototyping of complex shape objects such as engine brackets and air exhaust using laser bending has already been reported [9].

Laser bending mechanism

Two major mechanisms can drive the laser bending process, these are: temperature gradient and buckling [10,11]. The temperature gradient (TG) mechanism will be explained here as it was employed in bending the specimens in the present study. It operates whenever the laser beam is focused down to a diameter smaller than the thickness of the sheet to bend, as illustrated in figure 1. The scanning speed and power of the laser beam are such that a steep thermal gradient originates through the bulk of the metal, figure 2 (i). This results in differential thermal expansion through the thickness of the material underneath the beam spot, initially causing the sheet to counter-bend away from the heated surface, figure 2 (ii). Further heating reduces the mechanical properties (i.e. Young's modulus and yield stress) of the material and the bending moment of the sheet opposes the counter bending away from the laser beam [4]. The upper layer of the sheet continues to expand and becomes compressed against the surrounding cold material. When the temperature dependent yield stress is overcome by the thermal stress, the elastic compressive strain evolves into plastic strain. On cooling, the elastic portion of the strain is recovered back, yet the irreversible plastic strain makes the upper layer shorter than the bottom layer and an out of plane angle, i.e. 2θ, develops, figure 2 (iii). The bottom layer is hence mechanically strained and work-hardening may occur if the local temperature is less than the annealing temperature of the material. It must be emphasized that the temperature profile established by the TG mechanism must never exceed the melting point of the material during the process otherwise permanent damage occurs [8].

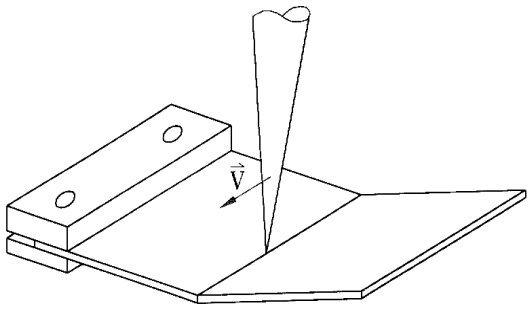

Figure 1. Schematic of laser bending by the TG mechanism (ref. 8)

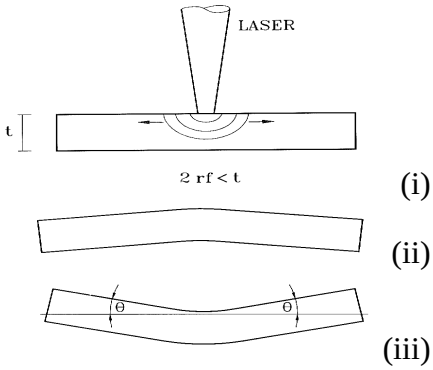

Figure 2. Sequence of events during the TG mechanism: (i) temperature gradient through the sheet, (ii) counter-bending (iii) final bend angle after cooling.

The angular deformation obtained every time the laser beam is scanned over the surface of the sheet is small; the bending angle increment is of the order of a few degrees per scan only [1,2,3,4]. If work-hardening takes place at the bottom layer, then the angle increment is decreased further as the number of scans increases, causing a characteristic decreasing-increments behavior of the bending angle when measured as a function of the number of scans (i.e. 2θ-N curves) [7]. For instance, in order to obtain a 90º bend, multiple runs of the laser beam must be undertaken. Heating of the work piece can also be done by moving the laser beam along a higher order trajectory. For example, if the beam follows a spirally outwards path, then a spherical deformation of the sheet occurs.

A two-layer model

The variables which affect the temperature gradient mechanism can be divided into three groups: material, geometrical and energy variables such as: - the Young's modulus, yield stress, coefficient of thermal expansion, thermal conductivity, specific heat capacity and absorptivity - thickness and cross-sectional length (i.e. width) of the sheet - laser power, spot size and speed, respectively [10,11]. To obtain a certain shape from a flat sheet, numerical calculations of the laser bending process can help in determining the necessary path, focal spot size, intensity and speed of the laser beam. This has been proven to be a difficult task to perform, nonetheless a simple, yet useful and comprehensive analytical model for the bending process by the TG mechanism has been proposed by Vollersten [12]. In this, two-layer (TL) model, a sheet of thickness, t, is divided into two layers of equal thickness and it is assumed that the upper layer is heated by means of a laser beam and therefore experiences thermal expansion whereas the bottom layer does not, as it is assumed insulated from the top layer. Figure 3, shows how the top layer gets shorter by an amount, Δl, due to plastic compression, and the bottom layer whose original length, l, remains unchanged. Figure 4, illustrates how the bending angle, 2θ, develops, as the two layers must remain geometrically constrained at all times.

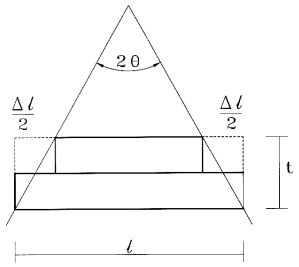

Figure 3. Geometry of the TL model.

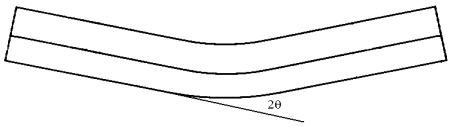

Figure 4. Schematic of the TL model final bend angle after cooling.

The bend angle increment, $\Delta\theta$, can be approximated to the overall compression, Δl, divided by the thickness, t. The overall compression can be estimated as the product of the thermal expansion, αl, and the change in temperature, ΔT:

$$\Delta\theta = \frac{\Delta l}{t} = \frac{\alpha \cdot \Delta T \cdot l}{t} \qquad (1)$$

The change in temperature can be obtained by considering the upper layer as a lumped system, hence:

$$\Delta T = \frac{\mathrm{P} \cdot \mathrm{A}}{\rho \cdot \mathrm{Cp} \cdot \mathrm{v} \cdot \frac{\mathrm{t}}{2} \cdot l} \tag{2}$$

By replacing equation 2 into 1, an expression for the bend angle increment is obtained, as follows:

$$\Delta\theta = \frac{2 \cdot \alpha \cdot \mathrm{P} \cdot \mathrm{A}}{\rho \cdot \mathrm{Cp} \cdot \mathrm{v} \cdot \mathrm{t}^2} \tag{3}$$

From equation 3, it can be predicted that the magnitude of the bend angle increment is directly proportional to the laser beam power, P (W), the coefficient of thermal expansion, α (1/K), and the absortivity to laser light, A, meanwhile its magnitude varies inversely proportional to the density, ρ (kg/m^3), heat capacity, Cp (J/kg/K), traversing speed, v (m/s), and to the square of the sheet thickness, t^2 (m^2). When all the parameters are held constant, this model predicts a linearly increasing bending angle with increasing number of scans, i.e $2\theta = \Delta\theta \cdot N$. The TL model can fit data from the initial scan stages of the process reasonably well, taking into consideration that it does not include the effects of counter-bending. Further number of scans will result in a non-linear behavior due to work- hardening and annealing effects [7, 8], which are also not included is this model.

Material properties issues

Low carbon steels have a bcc crystal structure, thus no stacking fault energy (γ_{SF}), whereas aluminum is an fcc material having a high γ_{SF} value. Austenitic stainless steels such as 304 series have also an fcc crystal structure and the highest value of the strain-hardening coefficient (n) of the three materials (i.e. lowest γ_{SF}). Table 1, shows a summary of the average values of different materials properties for these alloys.

	304 stainless steel	**1100 aluminum**	**1010 carbon steel**
Density (kg/m^3)	8030	2710	7871
Specific heat capacity (J/kg/K)	500	904	520
Heat conductivity (W/m/K)	22	222	53
Thermal diffusivity *10^6 (m^2/sec)	5.5	90.6	12.9
Melting temperature (K)	1723	916	1809
Thermal expan. coeff. (μm/m/K)	17.8	24.6	12.9
Young's Modulus (GPa)	193	69	199
Yield stress (MPa)	330	145	390

Table 1. Thermo-physical and mechanical properties values averaged over a 100-500 ^{o}C range (ref. 13).

Considering the following process parameters: v = 10 mm/s, P = 80 W, A = 0.7, and t = 0.5 mm, the expression for the angle increment given by equation 3, becomes:

$$\Delta\theta = 22.4{*}10^{9} * \frac{\alpha}{\rho \cdot \mathrm{Cp}} \tag{4}$$

It must be noticed that equation 4 does not include the effect of heat conduction, and therefore the results obtained from it are less likely to match the observed empirical results; for instance, when evaluated for 1100 aluminum, equation 4 gives angles that are almost 6 times larger than the empirical ones. Moreover, in equation 3, the thermal expansion length (i.e. length of material that experiences a sufficiently large ΔT, as to undergo plastic thermal compression) and thermal diffusion length are both taken to be equal to the cross-sectional length of the sheet, l, thus canceling out. By computing the following correction factor,

$$f = \frac{l_{\text{expansion}}}{l_{\text{diffusion}}} \tag{5}$$

where the thermal expansion length, $l_{\text{expansion}}$, is taken to be equal to the diameter of the laser focal spot and the thermal diffusion length, $l_{\text{diffusion}}$, is considered as twice the square root of the product of the thermal diffusivity and the laser-material interaction time. The bend angle increment can then be re-evaluated for these three materials, as shown below.

	304 stainless steel	**1100 aluminum**	**1010 carbon steel**
$\Delta\theta$ (deg)	5.7	12.9	4.0
f	0.43	0.11	0.28
$\Delta\theta$*f (deg)	2.4	1.4	1.1

Table 2. Bend angle increment, correction factor and re-calculated values using Eqs. 4 and 5.

Experimental Setup

Wrought sheets of dimension: 80 mm x 80 mm and 0.5 mm thick; made out of 304 stainless steel, 1100 aluminum, and 1010 steel were used as specimens. The samples were suspended in air, clamped at one side only, and scanned with a CO_2 laser beam (TEM_{00} and linearly polarized) for several times following a linear path, as shown in figure 5. The optical power of the laser beam ranged from 64 to 95 W, and the maximum speed achieved was 15 mm/s (out of the page). The laser beam was focused down to approximately 0.35+/-0.05 mm at the top-facing surface of the sheet, which had been previously sprayed with colloidal graphite in order to increase and homogenize the coupling of the optical energy. Forced convection nitrogen cooling was allowed in between scans to lower the temperature down to ambient level. By capturing the cross-sectional view of the sheet as it bends with a digital camera, the image files generated this way were processed in a CAD system to obtain the magnitude of the bending angle, after each scan, with an error of +/-0.5 deg. Figure 6, shows the results of three different material samples that were laser bent by scanning them 17 times along a linear path at a speed of 10 mm/sec and a laser beam power of 80 W.

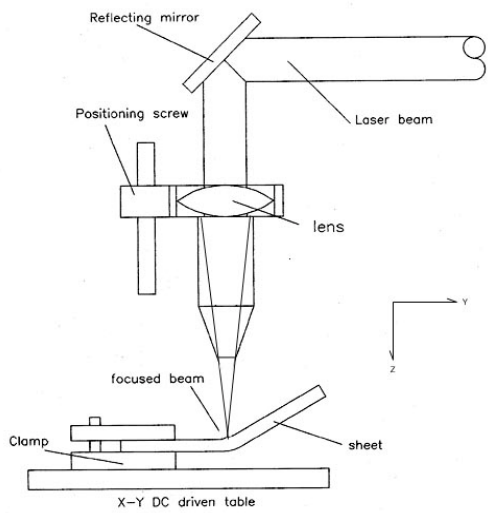

Figure 5. Experimental set-up for laser bending of thin metal sheets.

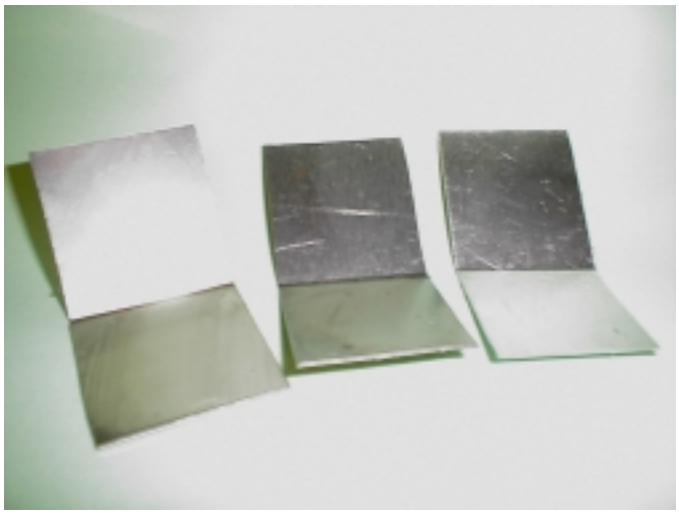

Figure 6. Laser bent thin metal sheets : 304 stainless steel (left), 1010 carbon steel (center), 1100 aluminium (right).

Results and Discussion

From figures 7, 8 and 9, it can be observed that as the optical power of the laser beam increases, keeping the scanning speed (v) and number of scans (N) constant, the bending angle also increases. 1100 aluminum appears to be more sensitive to laser power relative to 1010 steel, while 304 stainless steel shows the minimum relative increase in the bending angle with increasing power.

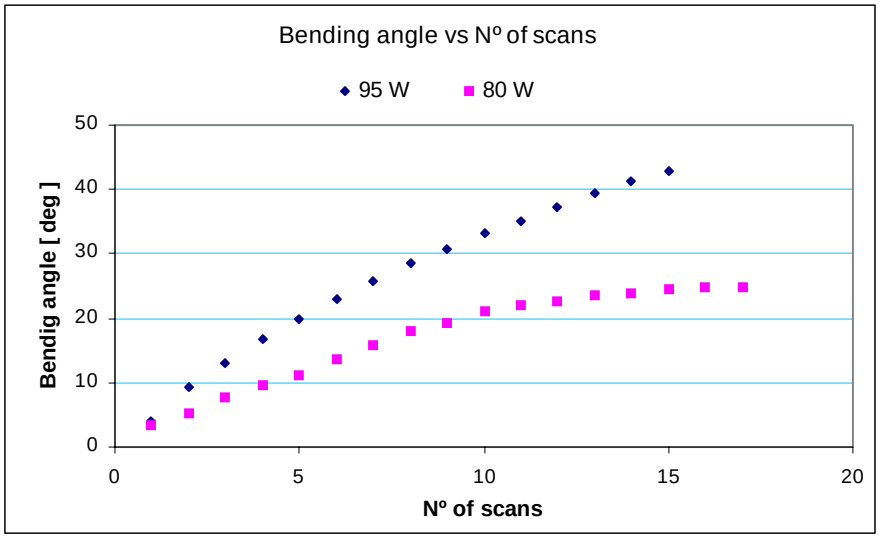

Figure 7. 2θ-N results for 1100 aluminum sheets bent at 10 mm/sec and two laser powers.

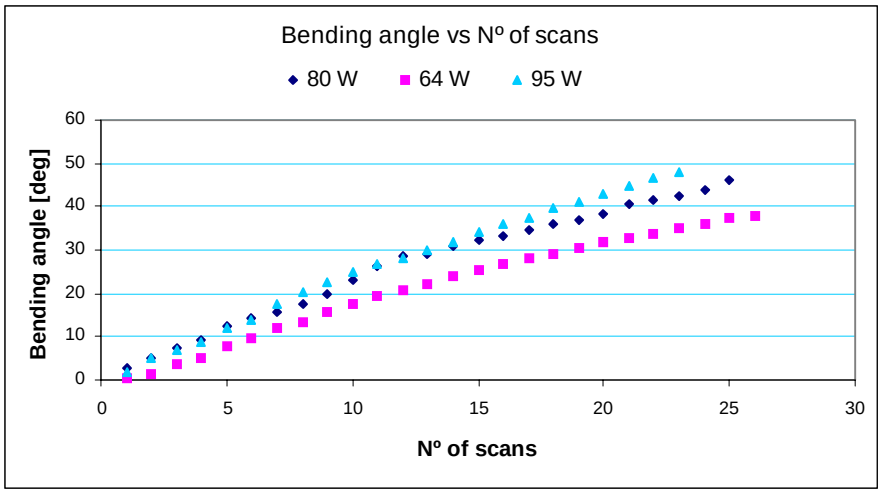

Figure 8. 2θ-N results for 1010 steel sheets bent at 10 mm/sec and three laser powers.

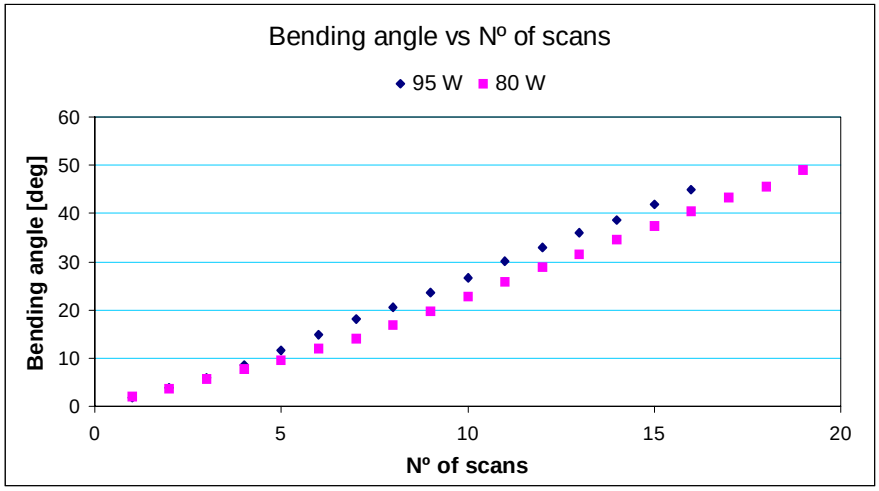

Figure 9. 2θ-N results for 304 stainless steel sheets bent at 10 mm/sec and two laser powers.

From the latter figures, the decreasing-increments behavior of the 2θ-N curve for 1100 aluminum and 1010 steel starkly contrasts with the increasing-increments behavior of 304 stainless steel. Examination of the empirical results obtained, showed that as the number of scans increases the bending angle increment (i.e. $\Delta\theta$) for 1100 aluminum and 1010 steel decreases in magnitude, whereas for 304 stainless steel, $\Delta\theta$ increases. This could be explained by the strain-hardening of the bottom layer of 1100 aluminum and 1010 steel samples, which may not become annealed. The thermal diffusivity of 1100 aluminum and 1010 steel is almost 17 and 7 times larger, respectively, than the value for 304 stainless steel. Meaning, that the heat flux entering these materials is rapidly conducted away towards the lateral cooler zones, creating a shallow thermal gradient that allows for the thermal expansion of the upper layer only, leaving the bottom layer at a temperature below the annealing temperature, 350ºC and 760 ºC, respectively [13]. On the contrary, the heat flux that enters the 304 stainless steel, builds up a deeper thermal gradient and then flows down to the bottom layer increasing the temperature, undegoing stress relief at 370 ºC and partial annealing at 1010 ºC [13].

304 stainless steel also shows the largest value of the strain-hardening coefficient of the three materials, thus dynamic recovery and partial recrystallization are prone to occur, as the dislocation density needed to drive these processes is sustained by the bending strains. Dynamic recovery and partial recrystallization relieve the strained layers from the effects of work-hardening facilitating further constant deformation [14].

Figure 10, illustrates the comparison of the bending behavior among the three materials when scanned at 10 mm/s and 80 W. It can be observed that up to the 4th scan, all three materials behave in a linear manner (i.e. $\Delta\theta$ is constant); 1100 aluminum and 1010 steel shows almost the same average angle increment values (i.e. 2.0 deg and 2.1 deg), whereas 304 stainless steel presents a slightly lower average value of 1.8 deg. When comparing these values with the ones obtained using the corrected TL model, it is possible to see that the angle increments are very close in magnitude, in despite of the fact that this time 304 stainless steel gives a larger angle increment, followed by 1010 steel and then 1100 aluminum. One possible reason for these results is that the thermal expansion length is assumed constant for the three materials and equal to the laser spot diameter. Beyond the 4th scan, aluminum shows the largest decrease in bending angle followed by low carbon steel. Instead, stainless steel shows an increasing-increments behavior of the angle. The explanation to this unexpected behavior, can be complemented with two additional facts: first, the heating cycles established during laser bending are generally short lived, as the total exposure time of the metal sheet to the laser beam, in this case, is 8 seconds per scan. Besides cooling down to room temperature is allowed in between the laser beam scans, making it less favorable for annealing to occurr in the 304 stainless steel. However, the second fact is that 304 steel has a low γ_{SF}, thus the creation of numerous stacking faults regions inside the rolled grains is possible. It is also known that stacking faults are responsible for the formation of annealing twins in this alloy. In the same way the reduction in dislocation density is a critical driving force for partial recrystallization, stacking faults of sufficient width and twins may increase the kinetics of recrystallization by acting as additional nucleation sites.

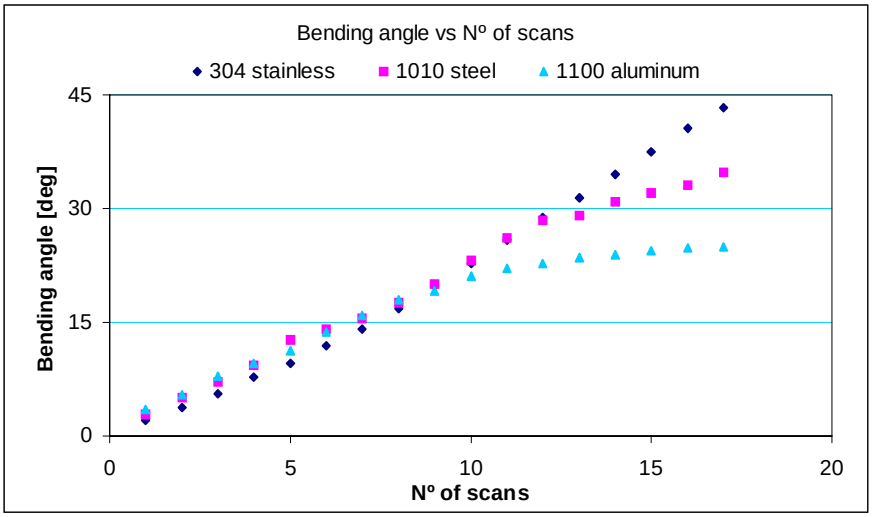

Figure 10. 2θ-N results for the three materials at 10 mm/s and 80 W.

These arguments can explain, for instance, why 304 stainless steel shows the largest bent angle after 15 scans (37.5 deg), followed by 1010 steel (32.1 deg) and then by 1100 aluminum (24.5 deg). The reason why 1100 aluminum develops a lower bent angle than 1010 steel may be found in its superior ability to strain-harden (i.e. fcc material). Moreover, its Young's modulus and yield stress are several times smaller than those of 1010 steel, and its coefficient of thermal expansion is almost twice that of the latter. Meaning, that 1100 aluminum will undergo more plastic deformation of the upper layer than 1010 steel will do under similar heat flux characteristics, yet at the same time, the straining of the bottom layer is larger, as well as its work-hardening. This is all under the assumption that the absortivity of the colloidal graphite coating over the sheets behaves similarly with the three materials.

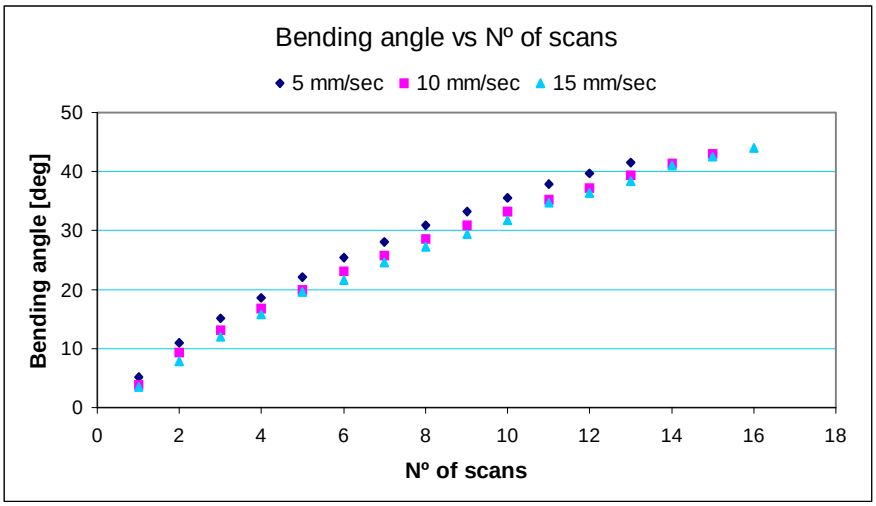

Figure 11. 2θ-N results for 1100 aluminum sheets bent at 95 W and three beam speeds.

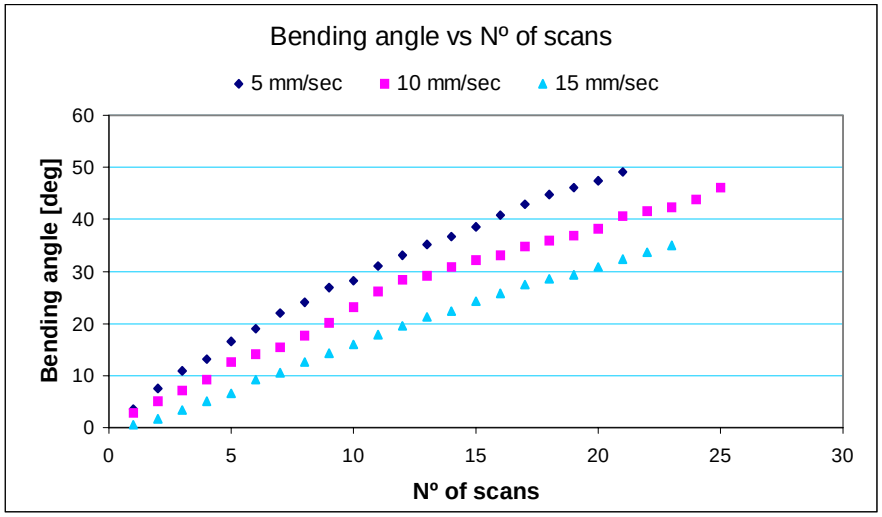

Figure 12. 2θ-N results for 1010 steel sheets bent at 80 W and three beam speeds.

When comparing the bend angle behavior of the three materials as a function of the scan speed (figures 11,12 and 13) it can be observed that 1100 aluminum shows the lowest sensitivity to deformation, followed by 1010 steel and then by 304 stainless steel. The latter material (figure 13) shows that for a bend angle of ~40 deg, 9 scans are required at 5 mm/s, whereas 23 scans are needed when the laser is scanned at 15 mm/s, both at 80 W.

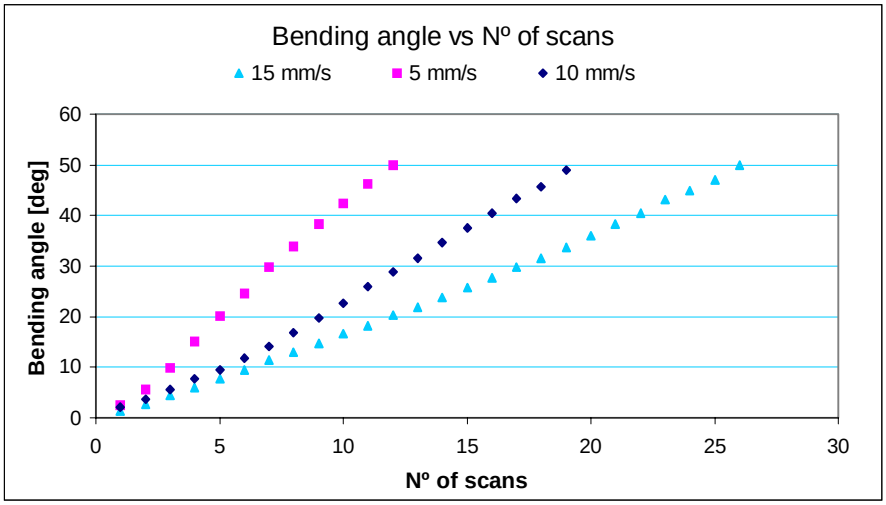

Figure 13. 2θ-N results for 304 stainless steel sheets bent at 80 W and three beam speeds.

Also from the three latter plots, it can be observed again that 1100 aluminum shows a marked decreasing-increments bending behavior that is unaffected by the scanning speed (figure 11). Its high thermal diffusivity causes the TG mechanism to operate regardless of the scanning speed even at 5 mm/s. For the 1010 steel, it can be noticed that a linear trend follows up to the 10^{th} scan and then a decreasing-increments behavior operates (figure 12). For 304 stainless steel, only at 5 mm/s it can be observed from figure 13, that a slight decreasing-increments curve develops beyond the 8^{th} scan; at low speeds the interaction time of the laser beam with the material is longer and so the temperature field penetrates through all the thickness of the material, probably causing the TG mechanism to no longer operate. On the other hand, at 10 and 15 mm/s the laser-material interaction times are shorter, making the thermal gradient shallower, yet its low thermal diffusivity allows the heat flux still to flow down to the bottom of the sheet, annealing the strained layers.

Finally, considering the number of scans and laser power fixed, all three materials show an inversely proportional decreasing trend of the bend angle with increasing speed as shown in figure 14. As the scan speed increases, the interaction time of the laser beam and the material becomes shorter; hence less energy enters the material. This makes the magnitude of the corresponding temperature field lower, which induces less thermal straining and thus less plastic deformation in the upper layer. Of the three materials, 304 stainless steel is the most sensitive to increasing the speed and 1100 aluminum is the least sensitive. Again, the large difference in thermal diffusivity between these two materials may explain such a behavior.

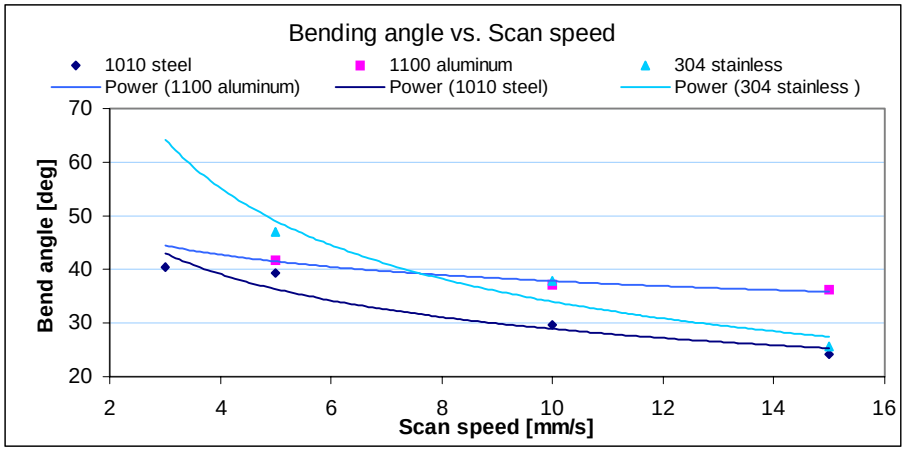

Figure 14. 2θ-scan speed results for three different materials at 80 W after 15 scans.

Conclusions

It was observed that after each laser scan was finished, all three types of thin metal sheets developed a bending angle towards the laser beam. The temperature-gradient mechanism is thought to be responsible for such a forming phenomena.

Numerical results, closer to the empirical values, are obtained when the two-layer model results are corrected by a dimensionless factor that takes into account the ratio of the thermal expansion length to the thermal diffusion length.

Increasing laser beam power increases the bending angle, whereas increasing scanning speed decreases it. 1100 aluminum shows a marked increasing bending angle sensitivity to increasing laser power and 304 stainless steel shows a decreasing bending angle sensitivity with increasing scanning speed. 1010 carbon steel is less sensitive to either laser power or scanning speed increase.

1100 aluminum and 1010 steel both show a decreasing-increments behavior of the bending angle (i.e. 2θ) evolution as the number of laser scans increase beyond the initial scans. The strain due to the as-received rolled condition of the sheets and in-situ strain-hardening during bending are not annealed by the laser heat flux due to its short lived thermal cycles and high thermal diffusivity of 1100 aluminum and 1010 steel. On the other hand, 304 stainless steel, shows an increasing-increments behavior of the bending angle instead. Strain-hardening is prone to occur in the latter material, however, stress relief and partial annealing may occur due to higher magnitude and longer time-scale thermal cycles. This is thought to be caused by 304 stainless steel low thermal diffusivity and possibly faster nucleation kinetics, due to a high density of stacking faults and twins, which may facilitate partial recrystallization.

Laser bending of thin metal sheets can be considered a rapid prototyping process as minimal tooling intervention is required and complex shapes can be formed from basic geometry preforms, e.g. thin sheets or tubes. Materials properties play an important role in determining the

process parameters needed to obtain a desired result with accuracy. This is important when determining in-control strategies in order to automate this kind of manufacturing process.

References

1. W.M. Steen, Laser Material Processing. Second edition. London: Springer–Verlag, 1998.
2. D. Schuocker, High Power Lasers in Production Engineering. London: Imperial College Press, 1999.
3. K.C. Chan, C. L Yau, W.B. Lee, "Laser bending of thin stainless steel sheets", Journal of Laser Applications, Vol. 12, No 1, 2000.
4. J. Magee, K.G. Watkins, W.M. Steen, "Advances in laser forming", Journal of Laser Applications, Vol. 10, No. 6, 1998.
5. J. Magee, K. G. Watkins, W. M. Steen, N. Calder, J. Sidhu, and J. Kirby, "Laser forming of high strength alloys", Journal of Laser Applications, Vol.10, No. 4, 1998, p149-155.
6. J. Magee, L.J. De Vin, "Process planning for laser assisted forming", 17th Irish Metals Conference, Galway, Ireland, August, 2000.
7. Sprenger, F. Vollertsen, W. M. Steen and K. G. Watkins, "Influence of strain hardening on laser bending", Manufacturing Systems 24, 1995, p 215-221.
8. J. Ramos, J. Magee, F. Noble, K. Watkins, W.M. Steen, "The microstructure of laser bent aluminium alloy AA2024-T3", in Proceedings of the 17th International Congress of lasers and Electro Optics (ICALEO 98), Orlando , 1998
9. F. Kloecke, A. Demmer, and C. Dietz, "Laser assisted metal forming, " in Laser Assisted Net Shape Engineering 2, Proceeding of the LANE`97, Vol. 2, p 81-92.
10. F. Vollertsen, M. Rodle, "Model for the temperature gradient mechanism of laser bending", Proceedings of the LANE'94, Vol. 1, 1994, p 371-378.
11. S. Holzer, H. Arnet, M. Geiger, "Physical and numerical modelling of the buckling mechanism", Proceedings of the LANE'94, Vol. 1, 1994, p 379-386.
12. F. Vollersten, "An analytical model for laser bending," Laser Eng. 2, 1994, p 261-276.
13. ASM Metals Handbook, 9th edition, Vol.1,2,3, Metals Park, Ohio.
14. M.E. Kassner, M.T. Perez-Prado, "Five power law creep in single phase metals and alloys", Progress in Materials Science, Vol. 45, 2000, Pergamon Press.